The Astrophysical Journal, 664: L115–L118, 2007 August 1

SOURCE OF NITROGEN ISOTOPE ANOMALY IN HCN IN THE ATMOSPHERE OF TITAN

Mao-Chang Liang,[1,2] Alan N. Heays,[3] Brenton R. Lewis,[3] Stephen T. Gibson,[3] and Yuk L. Yung[2]
Received 2007 May 7; accepted 2007 June 15; published 2007 July 12

ABSTRACT

The $^{14}N/^{15}N$ ratio for N_2 in the atmosphere of Titan was recently measured to be a factor of 2 higher than the corresponding ratio for HCN. Using a one-dimensional photochemical model with transport, we incorporate new isotopic photoabsorption and photodissociation cross sections of N_2, computed quantum-mechanically, and show that the difference in the ratio of $^{14}N/^{15}N$ between N_2 and HCN can be explained primarily by the photolytic fractionation of $^{14}N^{14}N$ and $^{14}N\,^{15}N$. The $[HC^{14}N]/[HC^{15}N]$ ratio produced by N_2 photolysis alone is 23. This value, together with the observed ratio, constrains the flux of atomic nitrogen input from the top of the atmosphere to be in the range (1–2) $\times$ 10^9 atoms cm^{-2} s^{-1}.

Subject headings: atmospheric effects — methods: numerical — molecular processes — planetary systems — planets and satellites: individual (Titan) — radiative transfer

1. INTRODUCTION

The explanation for the formation and evolution of Titan's massive N_2 atmosphere has remained a challenge since its discovery in the 1980s by *Voyager 1*. The discovery of the depleted $^{14}N/^{15}N$ ratio on Titan (Niemann et al. 2005; Waite et al. 2005), relative to those on the Earth (Fegley 1995) and Jupiter (Owen et al. 2001), implies that Titan experienced hydrodynamic escape of nitrogen (e.g., Lunine et al. 1999), similar to the hydrogen escape on paleo-Earth (Tian et al. 2005). The *Cassini-Huygens* mission observed depletion of the noble gases such as ^{36}Ar and ^{40}Ar (Niemann et al. 2005), relative to those on the Earth, suggesting that the primordial nitrogen was captured as NH_3 instead of N_2. Therefore, the isotopic composition of nitrogen provides a powerful constraint, not only on the formation and evolution of Titan's atmosphere but also on the evolutionary history of nitrogen compounds in the solar nebula (e.g., Owen et al. 2001).

The *Cassini-Huygens*-derived $^{14}N/^{15}N$ ratio in N_2 is 183 $\pm$ 5 (Niemann et al. 2005), but the ratio in HCN observed by ground-based telescopes (Marten et al. 2002; Gurwell 2004) is in the range ~60–110, depending on the temperature profile assumed in the data reduction. The explanation for the large difference between the $^{14}N/^{15}N$ ratios in N_2 and HCN on Titan provides yet another challenge for planetary science. The production of HCN is initiated by the dissociation of N_2 (Strobel & Shemansky 1982; Yung et al. 1984). Most of the known biogeochemical processes possess isotopic fractionations with magnitudes 1–100 permil (parts in a thousand), with the exception of O_2 photolysis at Lyα (Liang et al. 2007a), which enhances the yield of heavy $O(^1D)$ by as much as a factor of 10. Given that the $^{14}N/^{15}N$ ratio for N_2 is a factor of 2 greater than that for HCN, a process similar to O_2 Lyα photolysis is needed for the solution of this problem. In this Letter, with the aid of isotopic photoabsorption/photodissociation cross sections computed using an innovative quantum-mechanical molecular model, the photolytic fractionation of $^{14}N^{14}N$ and $^{14}N^{15}N$ is considered. We show that the large discrepancy in the $^{14}N/^{15}N$ ratio between N_2 and HCN can be explained readily to be driven primarily by photolytic processes in N_2.

2. ISOTOPIC CROSS SECTIONS

Extreme-ultraviolet (EUV) photoabsorption/photodissociation cross sections for $^{14}N^{14}N$ and $^{14}N^{15}N$, corresponding to the dipole-allowed electronic transitions from the $X\ ^1\Sigma_g^+$ ground state to the strongly coupled Rydberg and valence states of $^1\Pi_u$ and $^1\Sigma_u^+$ symmetry, have been computed quantum-mechanically using the diabatic coupled-channel (CC) Schrödinger equation (SE) technique (van Dishoeck et al. 1984). The particular CC model employed, which has been described elsewhere (Liu et al. 2007), is an extension of previous experimentally calibrated models (Haverd et al. 2005; Lewis et al. 2005), including not only the electrostatic couplings within the $^1\Pi_u$ and $^1\Sigma_u^+$ excited-state manifolds (Stahel et al. 1983; Spelsberg & Meyer 2001), but also rotational coupling between the manifolds, necessary for a correct description of Λ-doubling and rotational intensity effects, including *P*/*R*-branch interference in the $^1\Sigma_u^+$–$X\ ^1\Sigma_g^+$ transitions. In addition, a manifold of Rydberg-valence-coupled $^3\Pi_u$ states, spin-orbit-coupled to the $^1\Pi_u$ manifold, has been included, for a correct description of predissociation (Lewis et al. 2005; Haverd et al. 2005). In contrast to line-by-line methods, the total cross section for a given temperature is evaluated from individual CC rotational-transition cross sections, each computed over the full required wavelength range and then added together, weighted by appropriate Boltzmann factors. The quantum-mechanical CC technique is ideally suited to the computation of isotopic cross sections, which are notoriously difficult to measure experimentally, simply by changing a *single parameter*, the reduced molecular mass, in the CC-SE.

CC photoabsorption/photodissociation cross sections for $^{14}N^{14}N$ and $^{14}N^{15}N$ have been computed for use here over the range 82.7–100 nm, for temperatures of 100, 150, 200, and 300 K, with linear interpolation applied for intermediate temperatures in the photochemical calculations of § 3, which take into account the altitude dependence of temperature in Titan's atmosphere. The cross sections, computed on a grid with an average step size of ~0.0004 nm, have been modified to include the effects of Doppler broadening and correspond to infinite spectral resolving power. Since the photochemical calculations of § 3 require both photoabsorption and photodissociation cross sections, we derived the latter by correcting the photoabsorption

[1] Research Center for Environmental Changes, Academia Sinica, Taipei 115, Taiwan; mcl@rcec.sinica.edu.tw.

[2] Division of Geological and Planetary Sciences, California Institute of Technology, Pasadena, CA 91125.

[3] Research School of Physical Sciences and Engineering, Australian National University, Canberra, ACT 0200, Australia.

cross sections using the CC-computed predissociation quantum yields, determined on a rotational basis by comparison between the relevant predissociation and radiative line widths. Since almost all absorption by N_2 results in dissociation in this region, in practice corrections were necessary only for the b–$X(1, 0)$ and c'–$X(0, 0)$ bands, near 98.6 and 95.9 nm, respectively.

The CC photodissociation cross section for $^{14}N^{14}N$ at 150 K is shown in Figure 1 (*top*). In this work, a boxcar average smoothing algorithm with a width of 0.003 nm is applied to the calculated cross sections. The smoothed ratio of the cross sections for $^{14}N^{15}N$ and $^{14}N^{14}N$ is shown in Figure 1 (*middle, light curve*), emphasizing the structural complexity. Also shown in the figure (*dark curve*) is the same ratio with 0.1 nm smoothing, which greatly reduces the structural variation in the spectra, suggesting that high-resolution spectra are required in order for isotope-selective shielding effects to be represented properly. Full-resolution calculations, discussed below, indicate that a grid width of 0.003 nm is sufficient for the photochemical modeling in § 3. We note that while the present isotopic cross sections are expected to be very reliable at the longer wavelengths, and indeed are the only ones available, some higher Rydberg states have been omitted from the CC model, leading to greater uncertainties at the shorter wavelengths. However, considering the weaker dissociation in this region, this limitation is not expected to be of significance to the present application of the CC cross sections. For wavelengths <82.7 nm, the high-resolution (~0.006 nm full width at half-maximum [FWHM]) $^{14}N^{14}N$ photoabsorption and photodissociation cross sections of Shaw et al. (1992) have been employed to supplement the CC cross sections, with zero-point-energy (ZPE) shifting (Yung & Miller 1997) applied to estimate the photolytic fractionation associated with this wavelength region. This approximation is not important since photodissociation at wavelengths <82.7 nm contributes only 10% of the total.

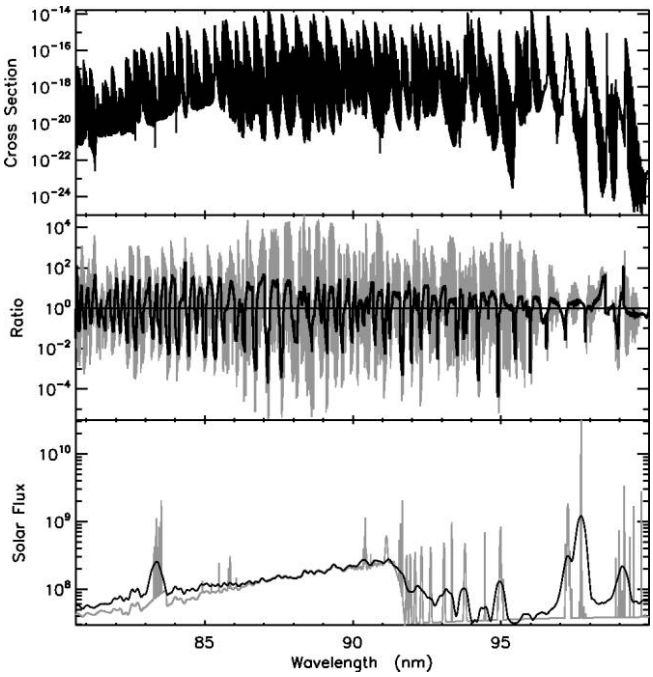

FIG. 1.—*Top*: Calculated CC photodissociation cross section (cm^2) for $^{14}N^{14}N$ at 150 K. *Middle*: Ratio of the smoothed photodissociation cross sections of $^{14}N^{15}N$ and $^{14}N^{14}N$ at 150 K (*light curve*, 0.003 nm smoothing; *dark curve*, 0.1 nm smoothing). *Bottom*: Observed (*dark curve*) and synthetic (*light curve*; see text) solar spectrum (photons cm^{-2} s^{-1} $Å^{-1}$), scaled at 1 AU.

3. PHOTOCHEMICAL MODELING AND RESULTS

The photolytic efficiency of an atmospheric molecule is related to the product of the incident solar flux and the molecular photodissociation cross section. Shifts in the ground- and excited-state rovibrational energies due to isotopic substitution cause corresponding shifts in the photoabsorption and photodissociation cross sections, which may result in significant differences in photolytic efficiency for the various isotopomers/isotopologues. In order for such photolysis-induced isotopic fractionation to occur, the incident flux must exhibit spectral structure, either naturally, for photolysis at the top of the atmosphere, or through structured atmospheric absorption, e.g., by molecular bands, in the case of photolysis at lower altitudes, or both. The case of the $O(^1D)$ product in O_2 Lyα photolysis (Liang et al. 2007a) provides a classic example of an extreme isotopic fractionation caused by significant shifts in isotopic photodissociation spectra. In the case of interest here, isotope-selective shielding allows more dissociative photons for $^{14}N^{15}N$ to penetrate deeper into Titan's atmosphere, resulting in higher photolytic efficiency for $^{14}N^{15}N$ than for $^{14}N^{14}N$ and, therefore, leading to a higher $HC^{15}N$ production rate.

Vertical profiles of species important for HCN formation have been calculated using a one-dimensional photochemical model (Yung et al. 1984; Liang et al. 2007c). Vertical eddy mixing coefficients and nitrogen and hydrocarbon photochemical reactions are taken from the literature (Yung et al. 1984; Liang et al. 2007c). The temperature profile, transport, and physicochemical molecular processes are taken to be the same as in Liang et al. (2007c). The chemical reactions adopted in this work are a subset of those of Liang et al. (2007c): we consider hydrocarbon chemistry up to C_2 species and nitrogen chemistry up to HCN (i.e., N_2, N, CN, NH, and HCN). The modeled HCN abundance with this simplified chemistry agrees with that of Liang et al. (2007c) to within a factor of 2. The results presented here will be unaffected by the selection of either simplified or complete hydrocarbon and nitrogen chemistry, as long as chemical processes other than N_2 photolysis are isotopically neutral. The ratio of $^{14}N/^{15}N$ in N_2 in the lower atmosphere used in this work is 183 (Niemann et al. 2005). The solar spectrum used for the N_2 photoabsorption and photodissociation calculations, shown in Figure 1 (*bottom, dark curve*), is taken from the literature (Woods et al. 1998; Ribas et al. 2005), with a spectral resolution of 0.2 nm FWHM. We then interpolate the solar spectrum onto the 0.003 nm grid used for the photoabsorption and photodissociation cross sections of N_2.

The calculated photodissociation rates for $^{14}N^{14}N$ (*solid curve*) and $^{14}N^{15}N$ (*dashed curve*), corresponding to the wavelength range 80–100 nm, are shown in the left panel of Figure 2. The total photoabsorption rate of N_2 in the atmosphere of Titan is 1.9×10^8 molecules cm^{-2} s^{-1}, with photofragmentation of N_2 only accounting for ~67%. Unlike normal N_2, where the rate peaks at 930 km, the isotope-selective photodissociation moves the $^{14}N^{15}N$ maximum down to 820 km. The right panel of Figure 2 shows the profile of the ratio of the photodissociation coefficients (J-values, defined by the product of the attenuated UV flux and the photodissociation cross section of the species) for $^{14}N^{15}N$ and $^{14}N^{14}N$, demonstrating a maximum at 760 km. N_2 photolysis is thus a mechanism capable of driving large fractionations in the atmosphere of Titan. Subsequent chemical and dynamical processes act to reduce the fractionation in N and HCN (see below).

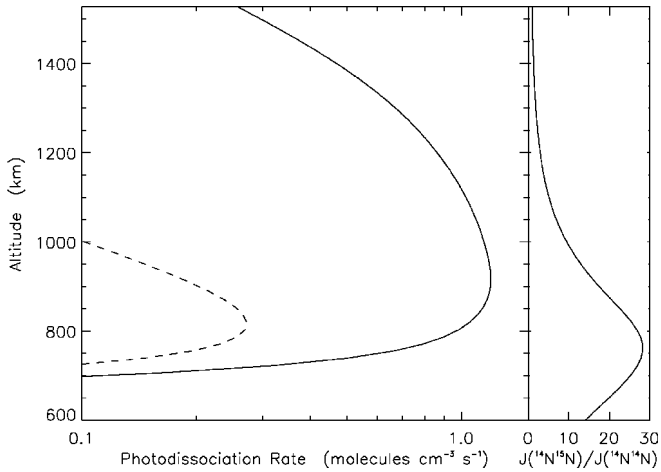

FIG. 2.—*Left*: Calculated photodissociation rates for $^{14}N^{14}N$ (*solid curve*) and $^{14}N^{15}N$ (*dashed curve*) in Titan's atmosphere. The additional absorption by CH_4 has been included in the calculations. These two species (N_2 and CH_4) are the major absorbers at wavelengths between 80 and 100 nm. *Right*: Ratio of the isotopic photodissociation coefficients.

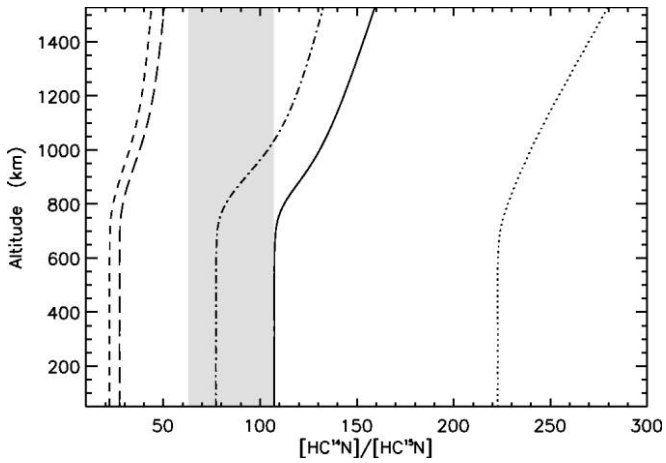

FIG. 3.—Modeled ratios of $HC^{14}N$ and $HC^{15}N$, with (*short-dashed curve*) and without (*dotted curve*) N_2 photolytic fractionation. The solid and dash-dotted curves represent modeled ratios for the cases of photolytic fractionation and an additional atomic nitrogen flux of 2×10^9 and 1×10^9 atoms cm^{-2} s^{-1}, respectively; the isotopic composition in this flux is assumed to be 183. The shaded area represents the observed range of $[HC^{14}N]/[HC^{15}N]$ (Gurwell 2004). For comparison, an approximate calculation based on ZPE-shifting the $^{14}N^{14}N$ spectrum (see text), which does not include nitrogen flux from the top of the atmosphere, is shown as a long-dashed curve.

The model-calculated ratios of the abundances of $HC^{14}N$ and $HC^{15}N$ in Titan's atmosphere are presented in Figure 3. A reference case that assumes no isotopic fractionation in the photolysis of N_2 yields the isotopic ratio given by the dotted line. The increasing nitrogen isotope ratio in HCN (also for other species such as N_2) above ~750 km, where the homopause is located, is caused by diffusive separation which depletes the abundance of heavy relative to light species. It is interesting to note that the ratio in the lower atmosphere is 223, a value greater than that (183) for N_2 in this region of the atmosphere. The greater isotopic ratio for HCN than for N_2 occurs because most of the HCN production takes place above ~800 km (Fig. 2), where its precursor, N_2, has a larger $^{14}N/^{15}N$ ratio.

The addition of $^{14}N^{14}N$ and $^{14}N^{15}N$ photolysis at wavelengths >80 nm (Fig. 1), in this case assumed to be the only source of atomic nitrogen, yields the short-dashed curve in Figure 3, corresponding to a ratio of $^{14}N/^{15}N = 23$ for HCN at lower altitudes. This large isotopic effect is caused primarily by the shifts in the rovibrational transition energies of N_2 due to isotopic substitution, together with associated differences in line intensities, including changes in nuclear-spin-mediated rotational intensity alternation and, to a lesser extent, predissociation yields. Also shown in Figure 3 (*long-dashed curve*) is the result of an approximate treatment in which the $^{14}N^{15}N$ cross section is estimated by ZPE-shifting the present CC cross section for $^{14}N^{14}N$. While the computed isotopic ratio in this case is reasonably close to the full-model value of 23, there is no reason to expect the ZPE-shifting technique to be valid in the case of highly structured coupled-states absorption spectra, such as for N_2. The magnitude of the photolytic fractionation suggests that other processes are required in order to reproduce the observed ratio of $^{14}N/^{15}N$ in HCN of ~60–100.

N_2 dissociation by cosmic-ray and Saturnian magnetospheric ion/electron impact provides an additional source of atomic nitrogen in the upper atmosphere of Titan. This source has been estimated to be 2×10^9 atoms cm^{-2} s^{-1} (Strobel & Shemansky 1982; Yung et al. 1984). If we assume that the $^{14}N/^{15}N$ ratio of atomic nitrogen produced by ion/electron impact equals that of N_2 at the top of the atmosphere (i.e., $^{14}N/^{15}N = 260$), the predicted $^{14}N/^{15}N$ ratio in HCN is 127. If the source is unaffected by molecular diffusion processes (i.e., $^{14}N/^{15}N = 183$), then $[HC^{14}N]/[HC^{15}N] = 107$. The actual value of $^{14}N/^{15}N$ in the atomic nitrogen source lies between 183 and 260. The strength of the source also affects the results presented here. Assuming $^{14}N/^{15}N = 260$ and a source strength of 1×10^9 (3×10^9) atoms cm^{-2} s^{-1}, the predicted $[HC^{14}N]/[HC^{15}N] = 86$ (151). Model results for fluxes of 1×10^9 and 2×10^9 atoms cm^{-2} s^{-1}, with $^{14}N/^{15}N = 183$, are shown in Figure 3 as dash-dotted and solid curves, respectively. This study of the sensitivity of the isotopic ratio to the strength of the N source constrains the input N flux to be (1–2) $\times 10^9$ atoms cm^{-2} s^{-1}, consistent with that derived previously.

The results presented above are sensitive to structural variations in both the solar and N_2 photodissociation spectra. In order to test the effect of the limited-resolution solar spectrum employed here, we have carried out a simulation using the full-resolution N_2 cross sections obtained in this work, together with a line-resolved synthetic solar spectrum (Fig. 1, *bottom, light curve*). This high-resolution spectrum is based on a semiempirical model of the emission of the Sun in the EUV, with spectral resolution on the order of 0.001 Å FWHM (D. E. Shemansky et al. 2007, in preparation), which is same as that used for transmission calculations in the atmosphere of Titan (Shemansky et al. 2005; Liang et al. 2007c). The full-resolution calculation reduces the calculated $[HC^{14}N]/[HC^{15}N]$ ratio by only 2%.

4. DISCUSSION

We have demonstrated that the large difference between the nitrogen isotope ratios observed in N_2 and HCN can readily be explained by the photochemical processes of $^{14}N^{14}N$ and $^{14}N^{15}N$, together with an additional source of atomic nitrogen, produced by cosmic-ray and Saturnian magnetospheric ion/electron-impact-induced N_2 dissociation, in the upper atmosphere of Titan. The main process driving the fractionation is isotope-selective shielding by N_2 that enhances the photolysis rate of $^{14}N^{15}N$ at lower altitudes. This process of modifying the dissociation rate of less abundant isotopomers/isotopologues is similar to those in the interstellar medium (ISM) (van Dishoeck

& Black 1988) and solar nebula (Lyons & Young 2005). Furthermore, the mechanism of ion-neutral chemistry that is proposed to fractionate the nitrogen isotope abundances in the ISM (Terzieva & Herbst 2000) can be ruled out as a primary source of nitrogen fractionation between N_2 and HCN in the atmosphere of Titan, for the following reasons. First, ion-neutral chemistry as a source of HCN accounts for only 40% of total production and is important only in the region above 1000 km (Wilson & Atreya 2004), while the $^{14}N^{15}N$ photolysis occurs mainly near 800 km. Second, the ion-neutral chemistry can only produce a fractionation less than 30% (Terzieva & Herbst 2000), which is insufficient to explain the difference between the observed $^{14}N/^{15}N$ ratios in N_2 and HCN.

By analogy with the $O + O_2$ isotopic-exchange reaction occurring during the formation of O_3 (e.g., Liang et al. 2006), one may speculate on the possibility of a similar $N + N_2$ reaction altering the strength of N-atom influx derived in this Letter. Such an isotopic-exchange reaction between N and N_2 could act to reduce the isotopic fractionation from N_2 photolysis, a role similar to that of the N influx. In order for this reaction to play a role, the rate coefficient has to be $>10^{-17}$ $cm^3\ s^{-1}$, a value that is very unlikely. The exchange of an N atom between N and N_2 is expected to be a slow process. Even though the formation of an intermediate N_3 radical is possible (Zhang et al. 2005), the N-N triple bond is too strong to be broken under the conditions prevailing in the upper atmosphere of Titan. An upper limit for the rate coefficient of the N-exchange reaction may be estimated by considering the reaction $H_2 + D \rightarrow HD + H$, for which the rate coefficient is $3.17 \times 10^{-10} \exp(-5205/T)$ $cm^3\ s^{-1}$, where T (K) is the temperature (Michael et al. 2004). Even at this upper limit, the exchange reaction is unimportant for N. A further possible mechanism for the enrichment of $HC^{15}N$ is the photoinduced isotopic fractionation effect in HCN itself, which can be calculated, e.g., based on ZPE shifting (Yung & Miller 1997; Liang et al. 2004). However, a preliminary estimate shows that the effect due to HCN photolysis is very small compared with the effect demonstrated here to result from the photolysis of N_2.

There remains a major challenge to explain the low $^{14}N/^{15}N$ ratio for N_2 in the atmosphere of Titan. In view of our success in explaining the isotopic composition of HCN, we believe that the resolution of the nitrogen isotopic fraction lies in (1) the photochemistry of NH_3 (Atreya et al. 1978), (2) the isotopic fractionation of ^{15}N in NH_3 photolysis (Liang et al. 2007b), and (3) hydrodynamic escape (Lunine et al. 1999; Tian et al. 2005). It is conceivable that some of the nitrogen in the primitive Titan might have been sequestered as HCN subduction to the interior of Titan, followed by conversion back to N_2, which would contribute to the isotopic enrichment of ^{15}N in the N_2 atmosphere.

This research was supported by NASA grant NNG06GF33G and *Cassini* grant JPL.1256000 to the California Institute of Technology, and Australian Research Council Discovery Program grants DP0558962 and DP0773050 to the Australian National University. Special thanks are due to D. Shemansky for providing a high-resolution solar spectrum. We also thank K. Dere, F. Mills, I. Ribas, and T. Woods for helpful discussion on the issue of the solar EUV flux, and N. Heavens and R. L. Shia for reading the manuscript. We thank W. DeMore, C. Miller, and H. Waite for valuable discussions on isotopic fractionation.

REFERENCES

Atreya, S. K., Donahue, T. M., & Kuhn, W. R. 1978, Science, 201, 611
Fegley, B. 1995, in Global Earth Physics: A Handbook of Physical Constants, ed. T. J. Ahrens (Washington: AGU), 320
Gurwell, M. A. 2004, ApJ, 616, L7
Haverd, V. E., Lewis, B. R., Gibson, S. T., & Stark, G. 2005, J. Chem. Phys., 123, 214304
Lewis, B. R., Gibson, S. T., Zhang, W., Lefebvre-Brion, H., & Robbe, J.-M. 2005, J. Chem. Phys., 122, 144302
Liang, M. C., Blake, G. A., Lewis, B. R., & Yung, Y. L. 2007a, Proc. Natl. Acad. Sci., 104, 21
Liang, M. C., Blake, G. A., & Yung, Y. L. 2004, J. Geophys. Res., 109, D10308
Liang, M. C., Cheng, B. M., Lu, H. C., Chen, H. K., Alam, M. S., Lee, Y. P., & Yung, Y. L. 2007b, ApJ, 657, L117
Liang, M. C., Irion, F. W., Weibel, J. D., Miller, C. E., Blake, G. A., & Yung, Y. L. 2006, J. Geophys. Res., 111, D02302
Liang, M. C., Yung, Y. L., & Shemansky, D. E. 2007c, ApJ, 661, L199
Liu, X., et al. 2007, ApJ, submitted
Lunine, J. I., Yung, Y. L., & Lorenz, R. D. 1999, Planet. Space Sci., 47, 1291
Lyons, J. R., & Young, E. D. 2005, Nature, 435, 317
Marten, A., Hidayat, T., Biraud, Y., & Moreno, R. 2002, Icarus, 158, 532
Michael, J. V., Su, M. C., & Sutherland, J. W. 2004, J. Phys. Chem. A, 108, 432
Niemann, H. B., et al. 2005, Nature, 438, 779
Owen, T., Mahaffy, P. R., Niemann, H. B., Atreya, S., & Wong, M. 2001, ApJ, 553, L77
Ribas, I., Guinan, E. F., Gudel, M., & Audard, M. 2005, ApJ, 622, 680
Shaw, D. A., Holland, D. M. P., MacDonald, M. A., Hopkirk, A., Hayes, M. A., & McSweeney, S. M. 1992, Chem. Phys., 166, 379
Shemansky, D. E., Stewart, A. I. F., West, R. A., Esposito, L. W., Hallett, J. T., & Liu, X. M. 2005, Science, 308, 978
Spelsberg, D., & Meyer, W. 2001, J. Chem. Phys., 115, 6438
Stahel, D., Leoni, M., & Dressler, K. 1983, J. Chem. Phys., 79, 2541
Strobel, D. F., & Shemansky, D. E. 1982, J. Geophys. Res., 87, 1361
Terzieva, R., & Herbst, E. 2000, MNRAS, 317, 563
Tian, F., Toon, O. B., Pavlov, A. A., & Sterck, H. D. 2005, Science, 308, 1014
van Dishoeck, E. F., & Black, J. H. 1988, ApJ, 334, 771
van Dishoeck, E. F., van Hemert, M. C., Allison, A. C., & Dalgarno, A. 1984, J. Chem. Phys., 81, 5709
Waite, J. H., et al. 2005, Science, 308, 982
Wilson, E. H., & Atreya, S. K. 2004, J. Geophys. Res., 109, E06002
Woods, T. N., Rottman, G. J., Bailey, S. M., Solomon, S. C., & Worden, J. R. 1998, Sol. Phys., 177, 133
Yung, Y. L., Allen, M., & Pinto, J. P. 1984, ApJS, 55, 465
Yung, Y. L., & Miller, C. E. 1997, Science, 278, 1778
Zhang, P., Morokuma, K., & Wodtke, A. M. 2005, J. Chem. Phys., 122, 014106